Broadband Ground Motion Simulation of an Intra-slab Earthquake Using a Hybrid Deterministic and Stochastic Aproach

Lawrence Livermore National Laboratory

Arben Pitarka

Lawrence Livermore National Laboratory, Livermore, CA

Abstract

1. In an effort to develop a methodology for simulating strong ground motion from intra-slab earthquakes we tested the broad-band ground motion simulation technique of Graves and Pitarka (2010) in modeling ground motion recorded from the M6.5 2010 Ferndale, California intra-slab earthquake.
The procedure is a hybrid technique that computes the low and high frequency parts of the ground motion separately, and then combines the two to produce a broadband time history. At frequencies below 0.8 Hz, the methodology is deterministic, and at frequencies above 0.8Hz up to 10Hz the ground motion is calculated using a stochastic representation of the source radiation and wave propagation. We then apply empirical site corrections based on the Vs30 to account for site effects (Campbell and Bozorgnia, 2012).
2. We analysed the performance of different 1D non-linear techniques in modeling the site response at the Humboldt bay geotechnical array under moderate shaking using recorded and simulated acceleration time hsitories of the 2010 Ferndale earthquake.

Findings

1. Graves and Pitarka (2010) broadband simulation method performed well at reproducing the ground motion from this intra-slab earthquake. In the simulation we used a stress parameter of 100. This is twice as high as the typical value of 50 used for simulating ground motion from strike-slip erthquakes in California
2. Comparisons of nonlinear and equivalent linear techniques results using strong motion data recorded at the geotechnical array indicate that for moderate input ground motion (peak acceleration of about 0.07g), the nonlinear (Bonilla et al., 2005) and equivalent linear methods give similar results. In addition, the comparisons of nonlinear results with the response under linear anelastic conditions indicate that soil nonlinearities may cause significant reductions, as high as 80%, in peak ground acceleration.

Graves, R. W. and A. Pitarka (2010). Broadband ground-motion simulation using a hybrid approach. Bull. Seism. Soc. Am., 100, 5A, 2095-2123.
Campbell, K. W., and Y. Bozorgnia (2008). NGA ground motion model for the geometric mean horizontal component of PGA, PGV, PGD and 5% damped linear elastic response spectra for periods ranging from 0.01 to 10 s, Earthquake Spectra 24, 139–172.
Bonilla, L., F., R. Archuleta, and D. Lavallee (2005). Hysteretic and dilatant behavior of cohesionless soils and their effects on nonlinear site response: field data, observations and modeling, Bull. Seism. Soc. Am., 95, 2373-2395.

2010 Ferndale, California Earthquake

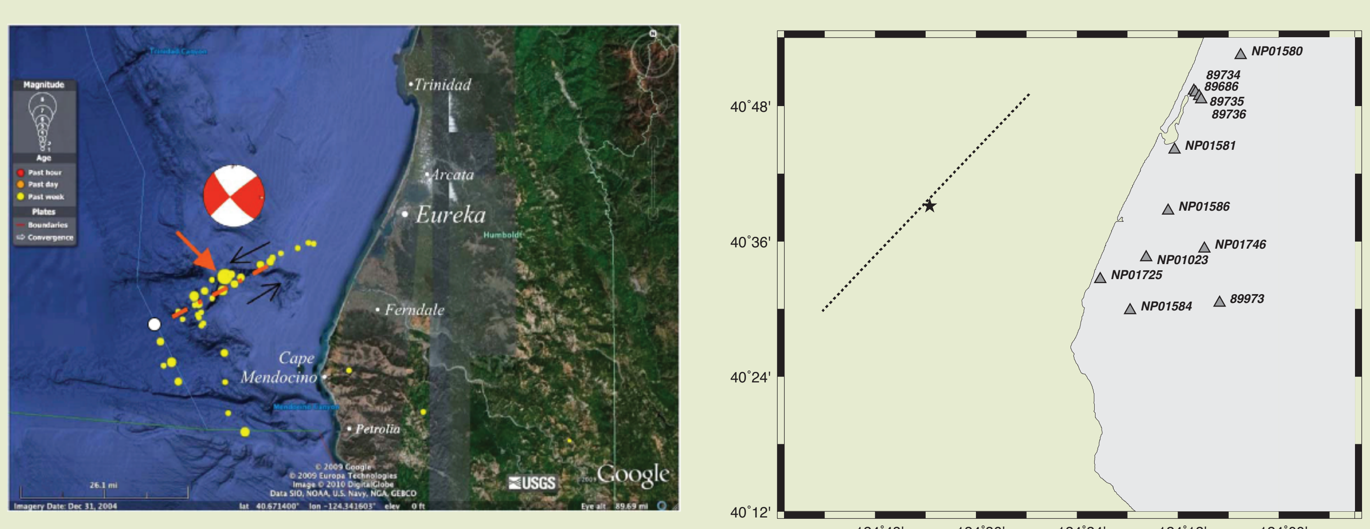

Figure 1.Left: Google map showing the largest aftershocks location. Arrow indicates the location of the epicenter. Right: Map of the study area showing the stations location (triangles), ocean-botto fault projection (dotted line), and epicenter location (star).

3D Velocity Model

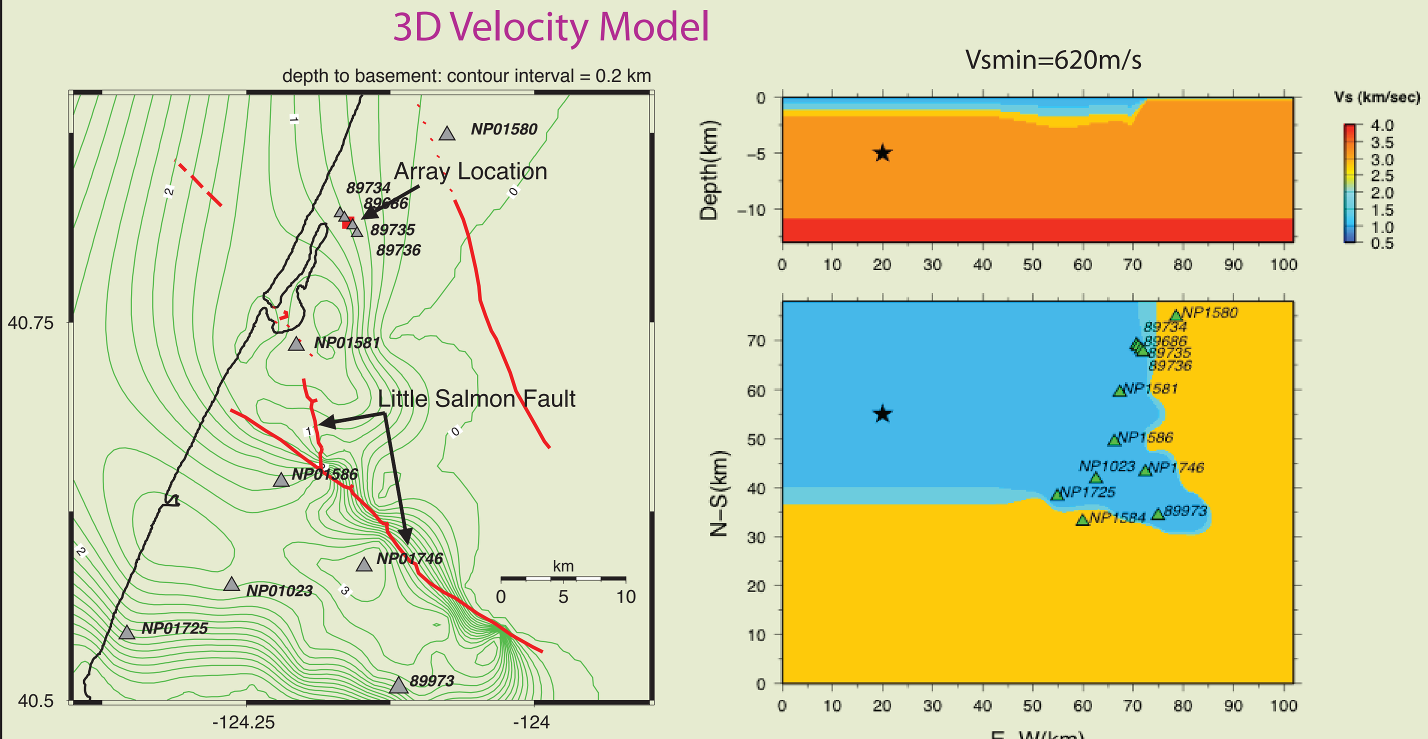

Figure 2.Left: Map of the basin depth. Green contour lines show depth to the basement, and red lines indicate location of major faults. The geotechnical array location is shown by the red square and indicated by the array, and the strong motion stations are shown by grey triangles. Right: W-E vertical cross section of the velocity model accross the epicenter (top panel) and free surface shear-wave velocity (bottom panel).

Kinematic Rupture Model

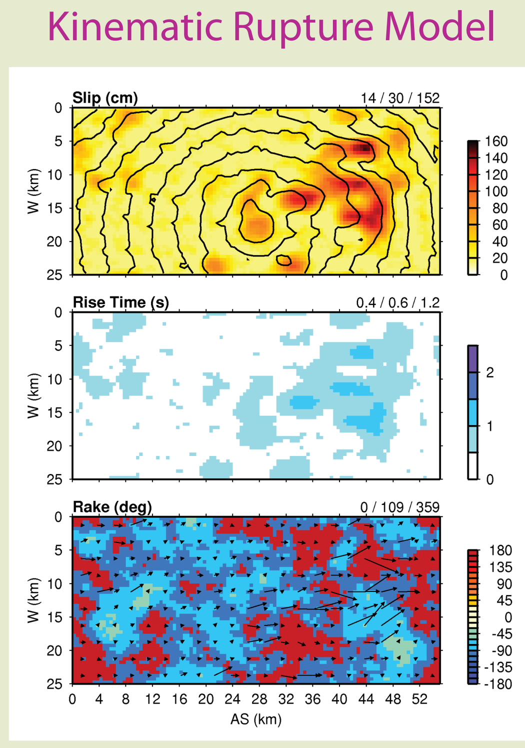

Mo=1.0x10^{25} dyne cm
Mw=6.6

Strike=230°; Dip 86°; Rake 11°

Depth-to-top = 10.5 km

Figure 3. Kinematic rupture model used in the broad-band simulations

Low Frequency Simulation Methodology (f<0.8Hz)

- Kinematic representation of heterogeneous rupture on a finite fault
  - Slip amplitude and rake
  - Rupture initiation time
  - Slip function
- Visco-elastic wave propagation using 3D FDM approach
  - MPI code
  - 3D velocity model
- Site-specific non-linear amplification factors based on Vs30

High Frequency Simulation Methodology (f>0.8Hz)

- Limited kinematic representation of heterogeneous rupture on a finite fault
  - Slip amplitude
  - Rupture initiation time
  - Conic averaged radiation pattern
  - Stochastic phase
- Simplified Green's functions for 1D velocity structure
  - Separate GFs for direct and downgoing rays
  - Amplitude decays as inverse of ray path length
  - Gross impedance effects based on quarter wavelength theory (Boore and Joyner, 1997)
- Site-specific non-linear amplification factors based on Vs30

Broadband Ground Motion Simulation (fmax=10 Hz)

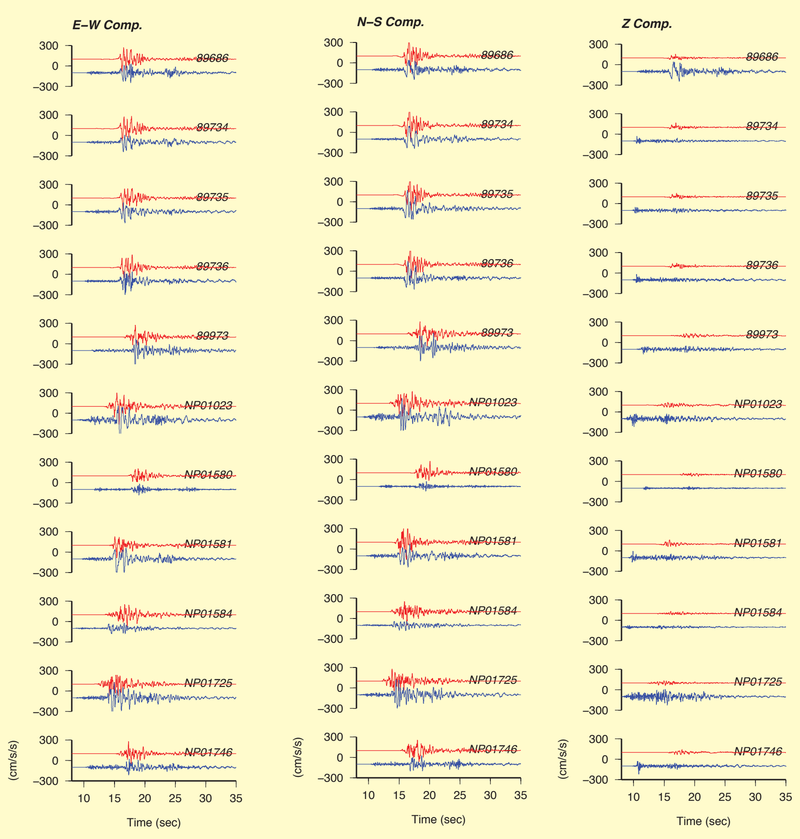

Figure 4. Comparison of simulated (red traces) and recorded (blue traces) ground motion acceleration

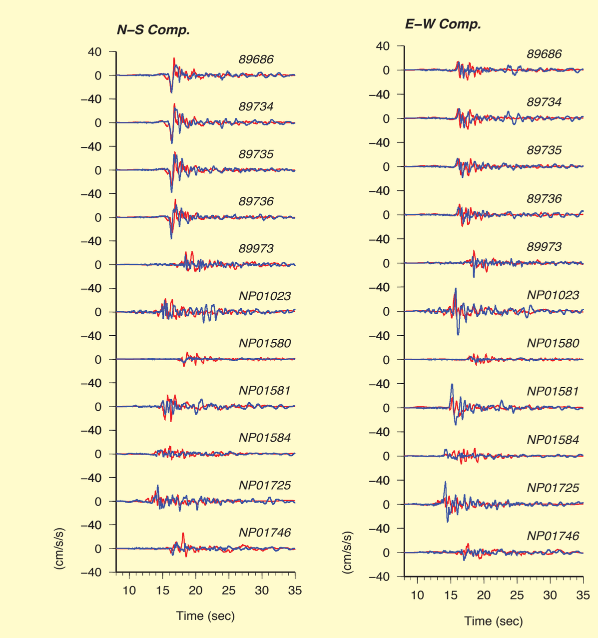

Figure 5. Comparison of simulated (red traces) and recorded (blue traces) ground motion velocity

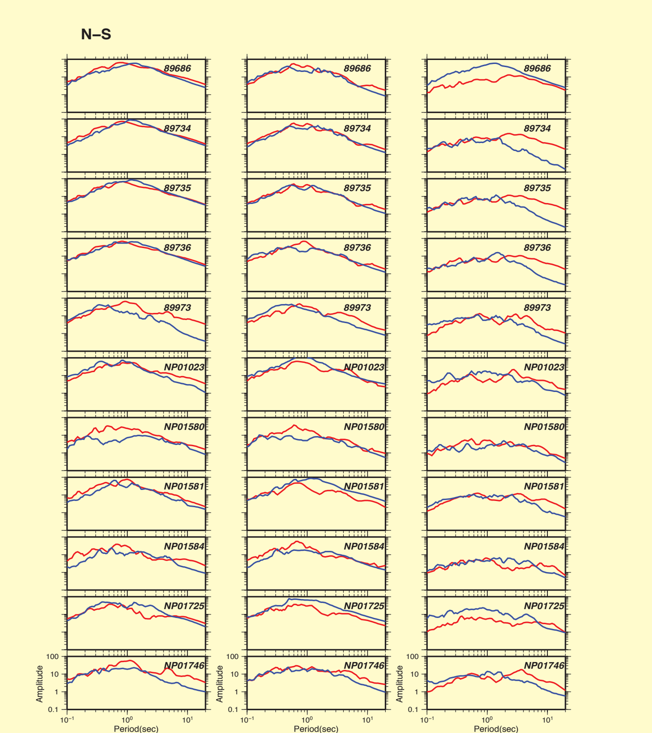

Figure 6. Comparison of simulated (red traces) and recorded (blue traces) ground motion acceleration response spectra

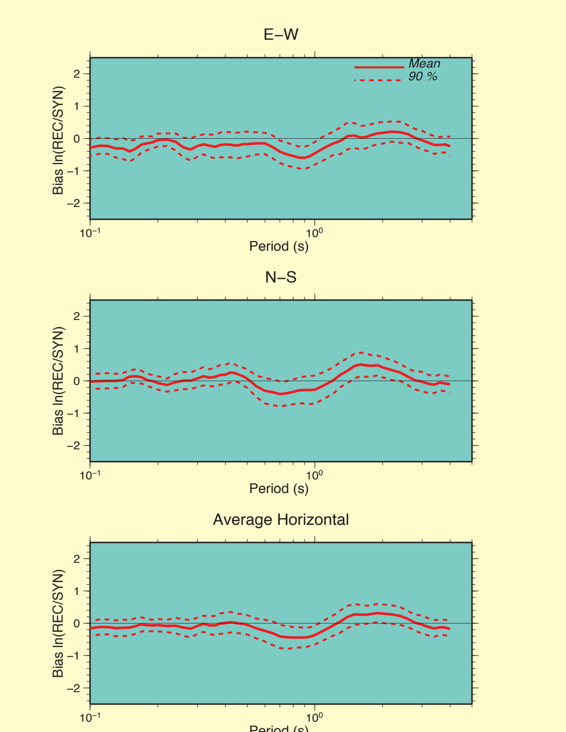

Figure 7. Model bias (heavy line) and standard error (area between dotted lines) for 5% damped spectral acceleration using 11 sites. Top panel shows the fault-parallel component, middle panel shows the fault-normal component, and bottom panel shows the average horizontal (geometric mean) component

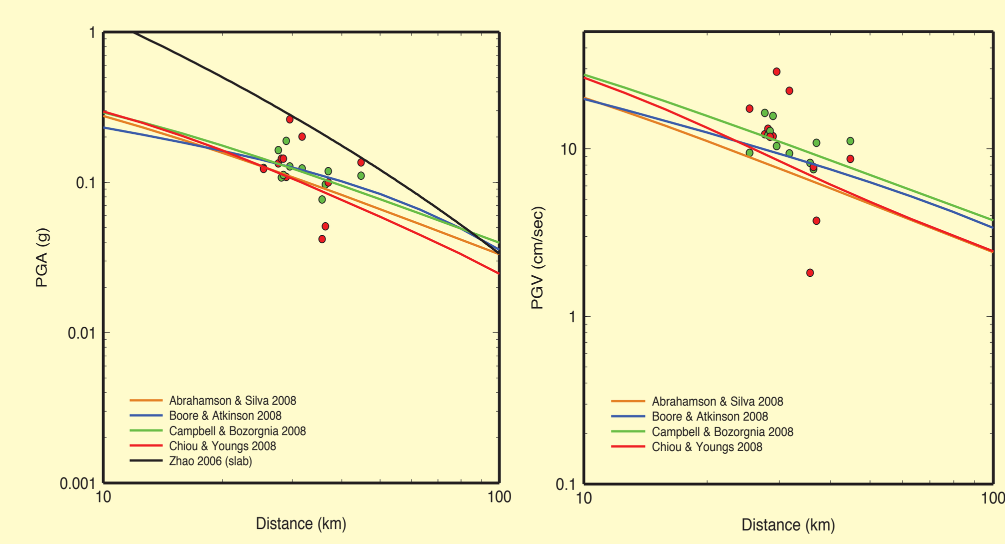

Figure 8. Comparison of simulated (green symbols) and recorded (red symbols) horizontal peak ground acceleration (left panel) and horizontal peak ground velocity (right panel) from the 2010 M6.5 Ferndale earthquake, with predictions using ground motion prediction equations.

Modelling Non-Linear Site Response at the Geotechnical Array (Bonilla et al., 2005)

Figure 9. Areal photo of the Humboldt Bay.
The geotechnical array (CSMIP Station No. 89734) is located less than 100m south-west of Eureka channel bridge

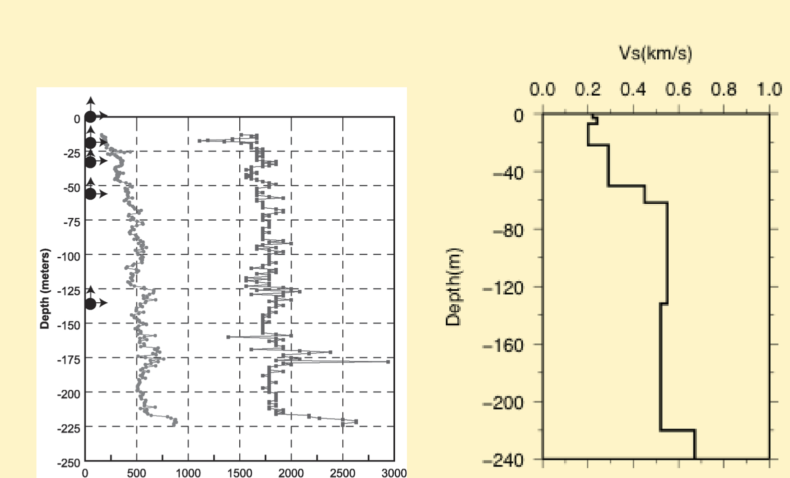

Figure 10. Left: Location of 4 borehole stations and velocity log data at the Geotechnical array. Right: 1D velocity model used in the non-linear soil response analysis.

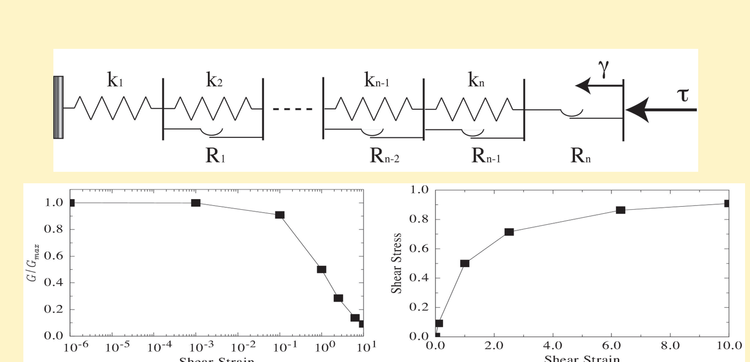

Figure 11. Non-linear soil resonse methodology (Bonilla, 2005) using Iwan-Mroz soil model (1967). Module reduction curces.

Fully Non-linear Method (Bonilla et al., 2005)

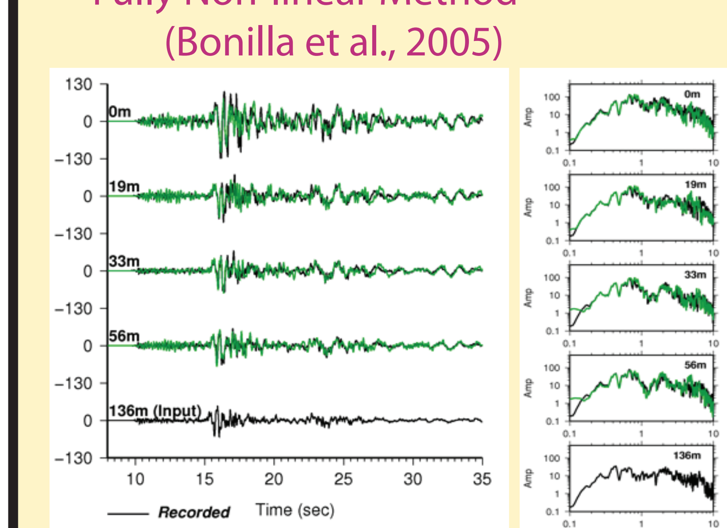

Figure 12. Comparison between recorded (black traces) and synthetic (green traces) E-W acceleration calculated at borehole stations using a fully non-linear technique. The input motion is applied at a depth of 136 m.

Equivalent Linear Method

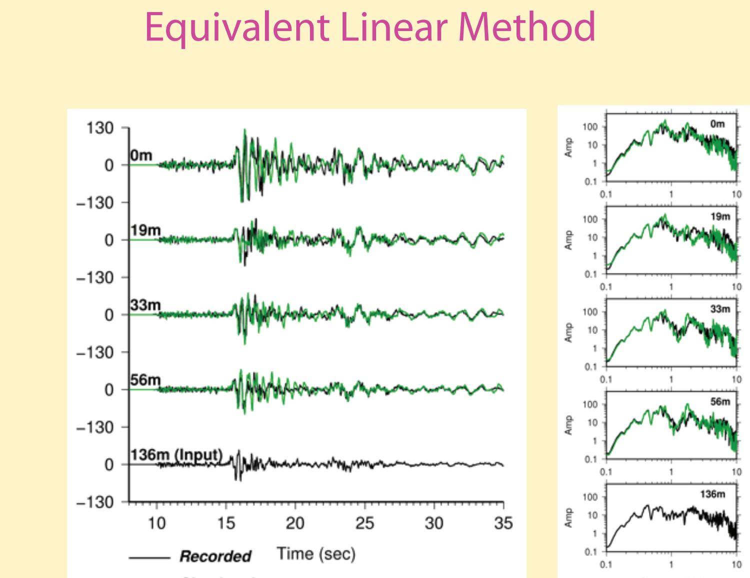

Figure 13. Comparison between recorded (black traces) and synthetic (green traces) E-W acceleration calculated at borehole stations using a equivalent linear technique. The input motion is applied at a depth of 136 m.

Linear Method

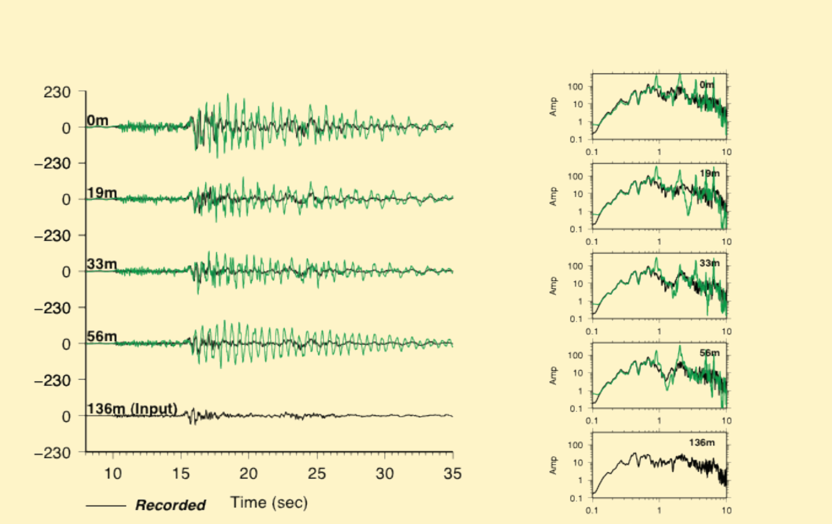

Figure 14. Comparison between recorded (black traces) and synthetic (green traces) E-W acceleration calculated at borehole stations using a fully non-linear technique. The input motion is applied at a depth of 136 m.

Performance of Vs30 Empirical Site Effects Correction

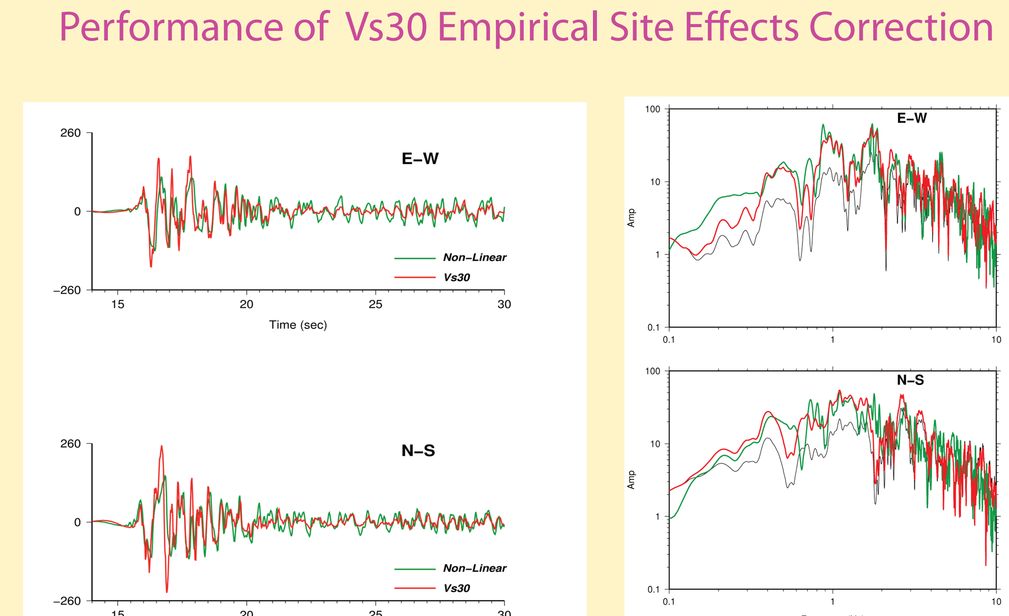

Figure 15. Performance of Vs30 empirical site effects correction at the geotechnical array. Comparison between the synthetic acceleration time histories (left panels) and corresponding amplitude spectra (right panels) calculated at the free surface using 1D nonlinear site response (green traces) and empirical site correction (red traces). Dotted line shows the amplitude spectrum of the input synthetic acceleration time history for the Ferndale earthquake model, applied at a depth of 136 m.

This work was performed under the auspices of the U.S. Department of Energy by Lawrence Livermore National Laboratory under Contract DE-AC52-07NA27344.